10356 2022 Session
SC A2 - Power Transformers & Reactors
PS 1 / Experience and new requirements for transformers for renewable generation

White-box Models Development for Insulation Design and Providing Transformers Withstand to High-Frequency Resonant Overvoltages

V.S. LARIN[1*], D.A. MATVEEV[2], M.V. FROLOV[2]
[1]All-Russian Electrotechnical Institute (VEI – branch of RFNC-VNIITF),
[2]Moscow Power Engineering Institute (NRU MPEI)
Russian Federation
vslarin@vei.ru

SUMMARY

Power transformers switching together with cable lines in renewable generation systems can be followed by high-frequency voltage oscillations affecting the insulation of that transformers. Under unfavorable conditions, when oscillation frequency is close to one of transformer winding natural frequencies, resonant overvoltages inside the winding can develop which leads to overstressing of windings internal insulation and the risk of transformer damage.

One of the possible measures to ensure the ability of transformer windings insulation to withstand operation high-frequency overvoltages is the application of high-frequency transformer models in order to determine dielectric stresses on windings internal insulation. At the stage of transformer insulation design and during design review within procurement process, it is extremely important to use high-frequency numerical models verified by comparison with experimental data.

For the development and verification of high-frequency power transformer models, experimental data regarding natural frequencies and damping factors of free oscillations inside windings is needed first.

This report describes an approach to the determination of natural frequencies and damping factors based on the registration of winding transient voltages and currents and fitting of free transient components with analytical equations. An approach to estimation of natural frequencies and damping factors using measured frequency responses of transformer winding is described too.

A method of inclusion of experimentally obtained damping factors into high-frequency models is presented; the method implies correction of eigenvalues of system matrix of ordinary differential equations system describing transients inside windings. An approach to the development of wideband transformer models is also presented which is correct for simulation on both high-frequency and low-frequency transients as well as steady states.

KEYWORDS

Power transformers, resonant overvoltages, windings, internal insulations stresses.

1. INTRODUCTION

In wind farms, the electric networks with connection of several wind generators into groups (clusters) by means of cable lines with the length from hundreds of meters to several kilometers are used.

Power transformers switching together with cable lines can be followed by the appearance of high-frequency oscillating voltages at transformer terminals; those voltages affect the internal insulation of that transformers' windings. Under unfavorable conditions, when oscillation frequency is close to one of transformer winding natural frequencies, resonant overvoltages inside that winding can develop which leads to overstressing of windings internal insulation and the risk of its damage.

Two main groups of possible measures to prevent winding insulation damage caused by resonant overvoltages can be highlighted:

1) application of protection equipment (RC-circuits installation, application of pre-insertion resistors in circuit breakers, etc.)

2) providing the ability of transformer windings insulation to withstand high-frequency overvoltages possible in operation.

The second group of measures requires the application of methods of investigation and simulation of high-frequency transients inside transformer windings to determine dielectric stresses at different parts of longitudinal insulation.

Recently, significant advances in high-frequency transformer modeling have been achieved. In the period from 2015 to 2021, CIGRE Working Group A2-C4.52 «High-Frequency Transformer and Reactor Models for Network Studies» carried out its activity. In 2019, the new Working Group «Transformer Impulse Testing» began its activity which includes simulation of high-frequency transients inside windings and estimation of transformers internal insulation stresses.

Detailed high-frequency transformer models based on design data, so-called white-box models [1], experienced huge development. They make it possible to estimate transformer natural frequencies and calculate qualitative picture of voltage distribution inside windings during high-frequency transients.

It is important to note that the reliability of high-frequency resonant transients simulation is determined by the accuracy of the representation of winding natural frequencies and damping factors in the model. In common, mathematical models used for simulation of impulse transients inside windings do not reproduce frequency dependency of the losses and damping at natural frequencies with enough accuracy as it is not crucial for impulse transients simulation.

Simulation of resonant transients inside transformer windings imposes high requirements to the accuracy of damping factor values as they determine resonant voltage rise ratios. The use of inaccurate values of damping factors can cause underestimation of transformer internal insulation stresses; this can lead to low safety factors and insufficient insulation withstand to high-frequency overvoltages possible in operation.

The authors of [2] suggest the approach to high-frequency transients simulation inside power transformer windings which is based on the use of the white-box model with lumped parameters determined from windings design data; this model should be supplemented by experimentally obtained values of damping factors. Such a hybrid model can be used for calculations both in the frequency domain, for example, for calculation of transfer functions of selected internal nodes, and in the time domain, for example, for calculation of induced voltages at transformer secondary windings [3].

In [4], an empirical expression is suggested for estimation of damping factors γ of natural oscillations at angular winding natural frequencies ω:

$$\gamma / \omega = 0{,}022 + 0{,}058 \cdot 10^{-6},\ \omega \le 0{,}5 \cdot 10^{6} \text{ rad/s}; \quad (1)$$

$$\gamma / \omega = 0{,}05,\ \omega > 0{,}5 \cdot 10^{6} \text{ rad/s}.$$

In [5], another expression can be found: $\gamma = (0{,}022 \pm 0{,}01)\omega$; this demonstrates significant dispesion of damping factor values obtained for different types of transformer windings.

At the stage of transformer insulation design and during design review within procurement process it is important to use high-frequency numerical models verified by comparison with experimental data. In [6], problems regarding confirmation of transformer ability to withstand high-frequency stresses are considered, the difficulty of such confirmation by means of high-voltage testing is pointed out, and an alternative to direct testing is suggested; that alternative is hybrid numerical and experimental confirmation which can be conducted by means of combination of low-voltage measurements and simulation using verified high-frequency transformer models.

For the development and verification of high-frequency power transformer models, experimental data regarding natural frequencies and damping factors of free oscillations inside windings is needed first. Such data can be obtained experimentally for transformers of identical or similar design.

2. EXPERIMENTAL DETERMINATION OF FREQUENCIES AND DAMPING FACTORS OF NATURAL OSCILLATIONS INSIDE WINDINGS

2.1. Determination of natural frequencies and damping factors from winding frequency responses

Frequency responses and voltage transfer functions are integral characteristics of power transformer windings characterizing geometrical parameters and electrical connections between different parts of the windings. Although these responses implicitly contain the information about frequencies and damping factors of winding natural oscillations, the process of their extraction is not trivial.

Approximate values of natural frequencies of transformer windings can be extracted from windings frequency responses using approaches [7, 8]. Main approaches are briefly described in table 1.

Table 1 – Approaches to natural frequencies determination

Approach	Advantages	Disadvantages
Based on local maximums of measured voltage transfer functions of winding internal nodes	Accuracy and simplicity. In case of deenergized tap changer (DETC) located in the middle height of the winding it is possible to obtain the values of 1st, 3rd and subsequent natural frequencies.	Availability of winding internal nodes is needed. For better determination of even natural frequencies, nodes at 1/4 and 3/4 of winding length or the lead from the last disk should be available which is commonly not possible in practice.
Based on local maximums of active component of winding input admittance	Accuracy of determination.	Utilization of vector network analyzers and high-frequency current transformers is needed which is not always available in practice. High-frequency current transformers usually have relatively narrow bandpass, which limits their application scope.
Based on local maximum of active component of winding admittance G_{12} determined from measured frequency response of the winding [7, 8]	The possibility of utilization of widely used Frequency Response Analysis (FRA) measurement equipment. Natural frequencies can be obtained as a by-product of FRA diagnostics measurements [9] performed within condition assessment of power transformer windings.	Not all natural frequencies are pronounced identically in frequency responses obtained from standard end-to-end measurements. It is necessary to use additional non-standard measurement schemes for more accurate determination of natural frequencies [10].

It should be noted that the approach based on frequency responses is somewhat approximate. In case of close natural frequencies or implicit resonance maximums this approach does not always allow one to determine winding natural frequencies with sufficient accuracy. However, this approach assumes

utilization of widely used FRA measurement equipment [9] which makes this approach more convenient and preferable for use in practice.

However, is it possible to determine damping factors of power transformer windings using frequency responses?

It is known from basics of electric circuits [11] that it is convenient to characterize the sharpness of resonance curve of input admittance, voltage or current of resonant circuit by its width $\Delta\omega$ at level of $1/\sqrt{2}$ of maximum value (–3 dB). In the case of the resonance curve of the circuit input current or input admittance the width $\Delta\omega$ is usually called the bandpass of the resonance circuit. For the common series RLC-circuit, the bandpass is inversely proportional to the quality factor: $\Delta\omega \approx \omega_{res} / Q = 2\gamma$, where ω_{res} stands for resonance angular frequency, and Q is the quality factor. In practice, this allows one to determine approximately the damping factor γ of a simple oscillating circuit using results of measurement of resonance circuit input admittance frequency response: $\gamma \approx \Delta\omega / 2$.

In [12], based on the consideration of simplified equivalent circuit of the transformer winding consisting of two pi-sections, analytical expressions were obtained for frequency dependency of voltage at the middle point, for active components of input admittance and for neutral current as well as for the relationship between widths of resonance peaks $\Delta\omega$ and damping factor γ, namely:

- for absolute values of voltage at internal nodes of the winding: $\gamma \approx \Delta\omega / 2$;

- for active component of input admittance and neutral current and reactive component of voltage at internal nodes of the winding: $\gamma \approx \Delta\omega / 2\sqrt{\sqrt{2}-1} \approx \Delta\omega / 1{,}3$.

Results presented in [12, 13] lead to a practically important conclusion about the possibility of damping factor estimation using expression $\gamma \approx \Delta\omega/1{,}3$ via determination of resonance peaks width $\Delta\omega$ of winding frequency response active component obtained from standard end-to-end measurements in accordance with IEC 60076-18 [9] and representing the ratio between neutral current and winding input voltage.

In [12, 13], it is shown that correct estimation of damping factor γ using resonance peaks width $\Delta\omega$ is possible, but far from always. The practical possibility of $\Delta\omega$ determination and the validity of γ estimation depend on how pronounced resonance peaks of frequency responses are and on how far adjacent winding natural frequencies are spaced. In the case of close natural frequencies, superposition of adjacent resonance peaks is possible which leads to incorrect estimation of $\Delta\omega$ and γ.

In general, frequency responses curves of neutral current active component have complicated traces. Resonance peaks may have both positive and negative polarity. For the calculation of the width of individual resonance peaks it is convenient to ignore information regarding their polarity and analyze absolute values. Calculation of the width of the individual resonance curve can be performed as follows [13].

1. Determination of natural frequencies f_i ($i = 1 \ldots n$) based on local maximums of resonance curve.
2. Determination of frequencies $f_{\min.i}$ ($i = 1 \ldots n + 1$) corresponding to local minimums of the curve in frequency ranges (0; f_1), (f_1; f_2), …, (f_{n-1}; f_n).
3. Determination of local maximums of resonance curve $A_{\max.i}$ in frequency ranges ($f_{\min.i}$; $f_{\min.(i+1)}$).
4. Determination of frequencies $f_{\text{left}.i}$ и $f_{\text{right}.i}$, within which resonance curve excceds $A_{\max.i} / \sqrt{2}$.
5. Calculation of resonance curve width:

$\Delta\omega_{left.i} = 2\pi(f_{left.i} - f_1)$; $\Delta\omega_{right.i} = 2\pi(f_{right.i} - f_i)$; $\Delta\omega_i = \Delta\omega_{right.i} - \Delta\omega_{left.i}$.

The described approach is illustrated below on the example of 1600 kVA power transformer with HV winding having cast insulation. Figure 1 shows frequency responses of phase A of the HV winding obtained from standard end-to-end measurements and corresponding frequency responses of conductance G_{12}. Figure 1, b illustrates that a good agreement of G_{12} curves in cases of open and closed LV winding starts from about 200 kHz which points out to the fact that the first HV winding natural frequencies are located in that region.

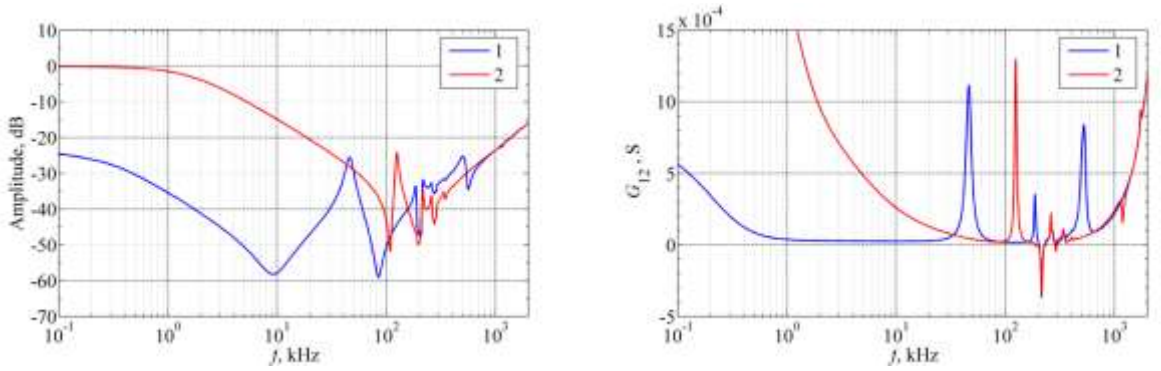

a) *b*)

Figure 1 – Frequency response (a) and conductance (b) of HV winding of 1600 kVA dry-type transformer in case of open (1) and closed (2) LV winding

Figure 2 shows the absolute value and active component of HV winding neutral current I_N for phases A, B and C obtained from measured frequency responses divided by Z = 50 Ohm.

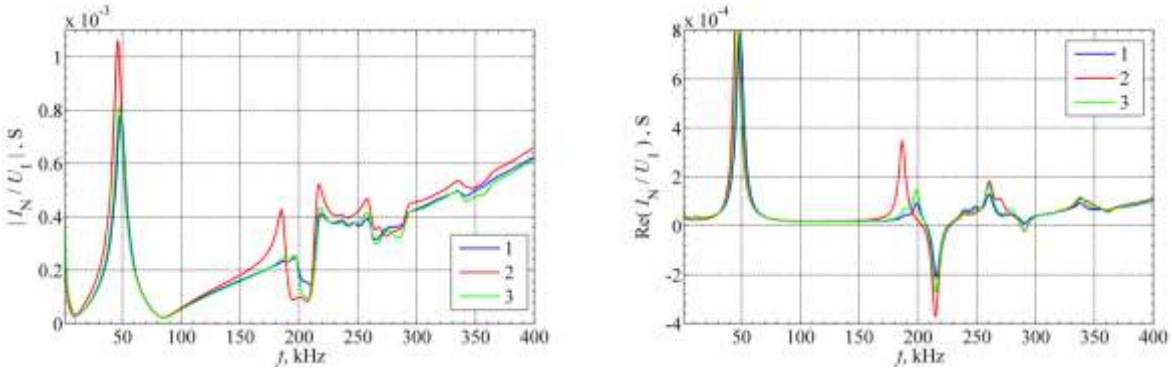

a) *b*)

Figure 2 – Absolute value (a) and active component (b) of HV winding neutral current I_N in case of open LV winding: 1, 2 and 3 – pahse A, B and C correspondingly

Figure 2 illustrates that resonance peaks in the active component of I_N are more pronounced than in absolute value of I_N. As seen from resonance peaks of the active component of I_N, the first natural frequency of HV winding is about 186 kHz, the second is about 200 kHz and the third is about 214 kHz. It should be noted that in active component of I_N of phase B the first natural frequency happens to be most pronounced while the second does not appear at all. For phases A and C, due to proximity of the first and the second natural frequencies, resonance peaks at the first natural frequency happens to be pronounced weakly in active component of I_N. These differences can be associated with design features of windings of the transformer under consideration, namely with the influence of adjacent windings due to low HV winding capacitance to earth, close location of adjacent HV windings and star connection of HV and LV windings (measurements of HV winding frequency responses shown above were performed using standard scheme with floated open-circuited LV winding, for details see [10]). These examples show that it is not always possible to determine damping factors for all natural frequencies of interest using standard-scheme frequency responses. In this case, in order to obtain missing results, one can use frequency responses measured via non-standard schemes with earthed adjacent windings [10], as well as voltage transfer functions of windings internal nodes available for measurements (for example, DETC or OLTC taps).

In practice, instead of using the damping factor γ, it is convenient to use the ratio of time constant of damping $\tau = 1/\gamma$ to a period of resonance frequency $T = 1/f_{res}$; this ratio represents the rate of free oscillation damping at windings natural frequencies. Using obtained above relationships between $\Delta\omega$ and γ, it is possible to write an approximate expression for τ / T based on measured frequency responses:

$$\frac{\tau}{T} = \frac{f_{рез}}{\gamma} \approx \frac{f_{рез}}{\Delta\omega} K_\gamma, \qquad (2)$$

where K_γ = 2 in case of calculation based on frequency responses of input admittance module and internal nodes voltage module; $K_\gamma = 2\sqrt{\sqrt{2}-1}$ in case of calculation based on frequency responses of input admittance active component, internal nodes voltage reactive component or neutral current active component.

Table 2 summarizes the results of estimation of τ / *T* ratio for the first three HV winding natural frequencies of the transformer under consideration.

Table 2 – Results of estimation of τ / T ratio for 1600 kVA transformer

Approach	Phase of HV winding	τ / T ratio for natural frequency with number		
		1	2	3
Transient voltage fitting [14] (with two dominant frequencies)	A	8,46	9,28	—
	B	8,65	—	9,29
	C	8,45	9,37	—
Estmation using (2) for Re(I_N) curve	A	*2,07*	7,66	10,3
	B	8,37	—	9,59
	C	*2,28*	8,25	10,1
Estmation using (2) for voltage transfer function in middle point of the winding	A	6,72	8,07	10,7
	B	8,04	—	10,4
	C	6,58	8,66	10,1

Thus, in the case of pronounced resonance peaks in the neutral current active component curve, damping factor estimation using the ratio γ ≈ Δω/1,3 gives a good agreement with the results of more accurate approach [14].

To summarize, it should be noted that for verification of obtained values of γ it is reasonable to compare results for different phases of power transformer winding as well as the results from different resonance curves, for example, winding neutral current and voltage transfer functions of available winding internal nodes (OLTC or DETC taps).

2.2. Determination of natural frequencies and damping factors via curve fitting of transient voltages and currents waveforms

More accurate determination of natural frequencies and damping factors can be achieved with the use of the approach based on registration and subsequent curve fitting of waveforms of transient voltages inside power transformer windings and neutral current [14].

To explain that approach the transient voltages and currents in simplified equivalent circuit of the winding consisting of four pi-sections with lumped parameters (figure 3) are considered below.

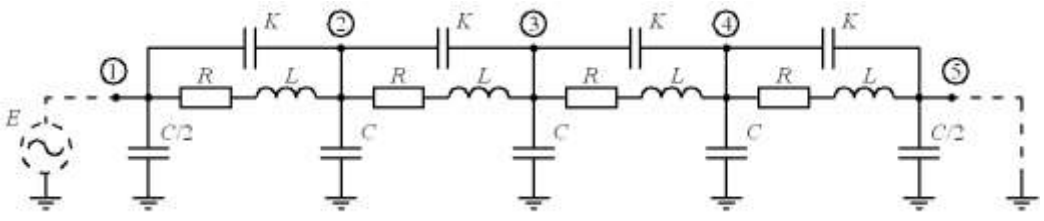

Figure 3 – Simplified equivalent circuit 4xRLC

In case of connection of the circuit from figure 3 to the source of unity sinusoidal voltage, expressions for voltage U_4 and neutral current I_N in operator form can be formulated as follows:

$$U_4(p) = \frac{\omega}{p^2+\omega^2} \cdot \frac{(pK(R+pL)+1)^3}{F_3(p)} \qquad (3)$$

$$I_N(p) = \frac{\omega}{p^2+\omega^2} \cdot \frac{(pK(R+pL)+1)^4}{F_3(p)\cdot(R+pL)} \qquad (4)$$

where

$$F_3(p) = \left(p(K+C)(R+pL)+1\right)^2 \cdot \left(p(4K+C)(R+pL)+4\right) + pC(R+pL)\left(pK(R+pL)+1\right)^2 \qquad (5)$$

Expressions for voltages at nodes 2 and 3 can be obtained in similar way.

It is important to note that the denominator of neutral current expression (4) of the 4xRLC equivalent circuit has common roots with denominators of expressions for internal nodes voltages. It can be shown that this is true for any degree of discretization of the considered equivalent circuit. In general, in the case of NxRLC equivalent circuit with $N \to \infty$, expressions for voltage at last winding element and neutral current can be formulated in general terms:

$$U_N(p) = \frac{F_1(p)}{F_2(p)} \rightarrow I_N(p) = \frac{U_N(p)}{Z(p)} = \frac{F_1(p)\cdot(1+pK(R+pL))}{F_2(p)\cdot(R+pL)}$$

Roots of 6th degree polynomial $F_3(p)$ are three complex conjugate pairs. Roots of denominator in (3) can be represented as the set of values:

$$p_{1,2} = \pm j\omega;\ p_{(2i+1),(2i+2)} = -\gamma_i \pm j\omega_i .$$

In time domain, expressions for voltage $u_4(t)$ and neutral current $i_N(t)$ can be expressed as follows:

$$u_4(t) = B_1 \sin\omega t + B_2 \cos\omega t + \sum_{j=1}^{3}\left(B_{2j+1}\sin\omega_i t + B_{2j+2}\cos\omega_i t\right)\cdot e^{-\gamma_j t} \qquad (6)$$

$$i_N(t) = D_1 \sin\omega t + D_2 \cos\omega t + \sum_{j=1}^{3}\left(D_{2j+1}\sin\omega_i t + D_{2j+2}\cos\omega_i t\right)\cdot e^{-\gamma_j t} + D_0 e^{-2\gamma_0 t} \qquad (7)$$

where B_1, B_2, D_1 и D_2 are the amplitudes of voltage and neutral current forced components; B_{2j+1}, B_{2j+2}, D_{2j+1} и D_{2j+2} are the amplitudes of voltage and neutral current free components with the frequency equal to j-th natural frequency of the circuit f_j; $\omega_j = 2\pi f_j$; D_0 is the initial value of an aperiodic component of neutral current.

From (6) and (7), practically important conclusion about the possibility of natural frequencies f_j and damping factors γ_j determination from free components of winding internal voltages and neutral current follows.

It should be noted that the considered 4xRLC network has three independent nodes which determines the presence of three natural frequencies. Real power transformers windings possess a higher number of natural frequencies, however, even in that case transient voltages and neutral current of the winding can be expressed by equations (6) and (7) with separation of oscillations into free and forced components.

The theoretical background presented above can be used in practical cases as follows. If internal nodes of power transformer winding, for example, taps of DETC or OLTC, are available, registration of transient voltages inside winding after connection of undamped sinusoidal voltage source with frequency of interest can be performed. Based on the representation of transient voltage inside windings as a superposition of free and forced components, the transient voltage can be approximated using expression of type (6).

In general, depending on source frequency, free oscillation can contain several natural frequencies. In common, first several natural frequencies are of greatest interest in the analysis of impulse and resonant transients inside transformer windings as they have the most substantial contribution in

transient voltages and are characterized by the highest voltage rise inside windings. Due to that, in practical cases, it is convenient to limit the number of considered natural frequencies to two or three featuring the highest amplitudes as they make a decisive contribution to transient voltage.

Fitting of transient voltage $u(t)$ inside winding can be done in the manner described below.

1. Determination of forced oscillations frequency f_0 and corresponding amplitudes B_1 and B_2 using steady-state part of the waveform. This can be done by determination of source frequency, the steady-state amplitude of voltage inside winding and phase shift between voltage inside winding and source voltage. Alternatively, one can do it using a least-squares method with f_0, B_1 and B_2 as independent variables. The second approach appears to be preferable due to less sensitivity to high-frequency noise superimposed on the signal.

2. Calculation of steady-state voltage approximation using determined values of f_0, B_1 and B_2 for the whole registered waveform of transient voltage: $u_{ss}(t) = B_1 \sin(2\pi f_0 t) + B_2 \cos(2\pi f_0 t)$.

3. Determination of free voltage component: $u_{free}(t) = u(t) - u_{ss}(t)$.

4. Spectral decomposition of free voltage component $u_{\text{free}}(t)$ using Fast Fourier Transform and determination of dominating natural frequencies as points of local maximums of the spectrum.

5. Determination of f_j, B_{2j+1} and γ_j values providing the best fitting of free component using least-squares method ($j = 1 \div n$, where n being a number of used frequencies). For example, in case of fitting with two frequencies, free component can be fitted with expression:

$u_{free}(t) = \left(B_3 \sin \omega_1 t + B_4 \cos \omega_1 t\right) \cdot e^{-\gamma_1 t} + \left(B_5 \sin \omega_2 t + B_6 \cos \omega_2 t\right) \cdot e^{-\gamma_2 t}$, где $\omega_1 = 2\pi f_1$ и $\omega_2 = 2\pi f_2$. As initial estimation of f_1 и f_2, natural frequencies with highest amplitudes in a spectrum of free component can be used.

6. Estimation of absolute fitting error $\delta U(t) = u(t) - u_{ss}(t) - u_{free}(t)$ and assessment of sufficiency of fitted frequencies number n.

Thus, the most pronounced natural frequencies can be obtained from spectral analysis of free component of transient voltage; these natural frequencies can be verified by means of free component fitting in the time domain.

Amplitudes of the free component spectrum at individual natural frequencies are more or less pronounced depending on how source frequency is close to considered natural frequency. Due to that, it is reasonable to select for transient voltage registration a number of source frequencies approximately equal to assumed natural frequencies and its intermediate values.

As an example, figures 4, a and 4, b show measured waveforms of HV winding middle point voltage (at DETC tap) of phase B of 1600 kVA dry-type transformer in case of source frequencies of 186 and 214 kHz (blue curves) and their approximation done in accordance with the algorithm described above (red curves). Figures 4, a, and 4, b illustrate the spectrum of voltage free component (blue curve) and the spectrum of source voltage (red curve). Frequencies of 186 and 214 kHz are approximately equal to the first and the third natural frequencies of HV winding. Transient voltages are given in relation to source voltage amplitude (5 V).

In this example, fitting of free component of transient voltage is done with two frequencies (f_1 and f_2). It is evident from figure 4 that in considered cases, when free voltage component contains one or two most pronounces natural frequencies, fitting error does not exceed 5%. In case of the presence of more natural frequencies with comparable amplitudes in free component spectrum it is can be reasonable to do free component fitting with more than two frequencies.

The principle of the algorithm described above is based on the extraction of forced voltage component. For that purpose, registration length should be sufficient to reach a steady state. Required transient registration time can be estimated using typical values of the time constant of damping inside windings. For power transformer windings, the ratio of damping factor γ to natural angular frequency ω is commonly $\gamma_i / \omega_i = 0{,}012 \div 0{,}032$ [3–5] which corresponds to the ratio $\tau_i / T_i \approx 5 \div 14$. Considering

that, registration time can be conservatively selected equal to 50÷100 periods of the first natural frequency (or its supposed value).

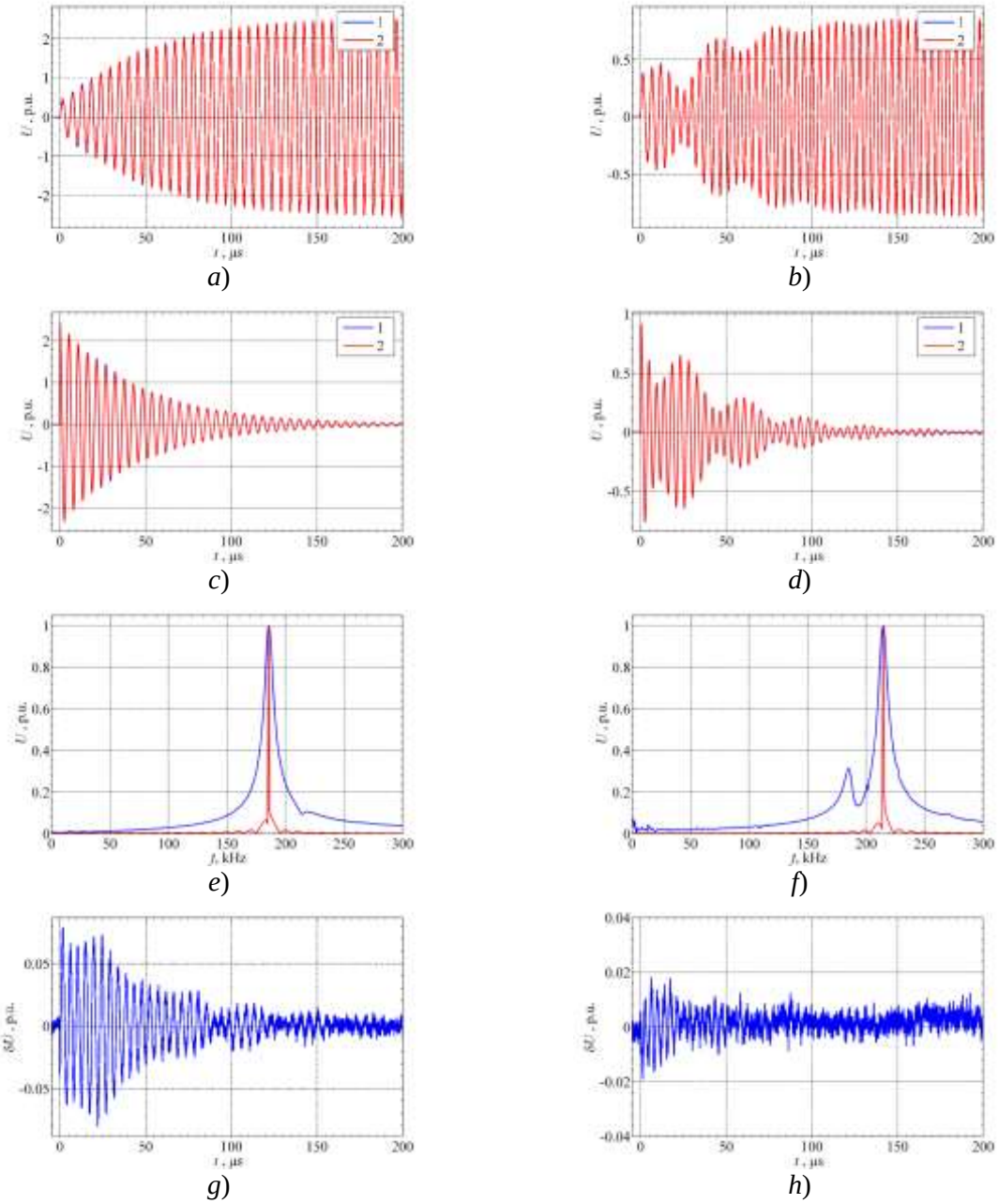

Figure 4 – Transient voltage (a, b), approximation (c, d), frequency spectrum (e, f) and absolute fitting error (g, h) of free voltage component at source frequency of 186 (a, c, e, g) and 214 kHz (b, d, f, h)

It should be noted that, in practice, winding internal nodes are not always available for measurements. This availability is possible when performing repetitive surge oscillography (RSO) in factory conditions which is usually done for new power transformers design with high rated power. Also, measurements at terminals of windings connected to DETC and OLTC are possible in practice, especially in case of dry-type transformers.

We now consider determination of natural frequencies and damping factors using neutral current registration.

For neutral current registration, current shunt of 50 Ohm matching impedance can be used. During measurement process, it must be kept in mind that neutral current at high frequencies and source

voltage of 5-10 V is of several of mA, so results of neutral current registration are more polluted with high-frequency noise than results of winding transient voltages registration.

Figures 5, a and 5, b show measured waveforms of HV winding neutral current of the transformer considered above at source frequencies at 186 and 214 kHz (blue curves) and the results of waveforms processing (red curves). Figures 5, e and 5, f show the spectrum of free current component (in blue) and resulting neutral current (in red). Transient currents are given in relation to 5 mA referred to 5 V source voltage.

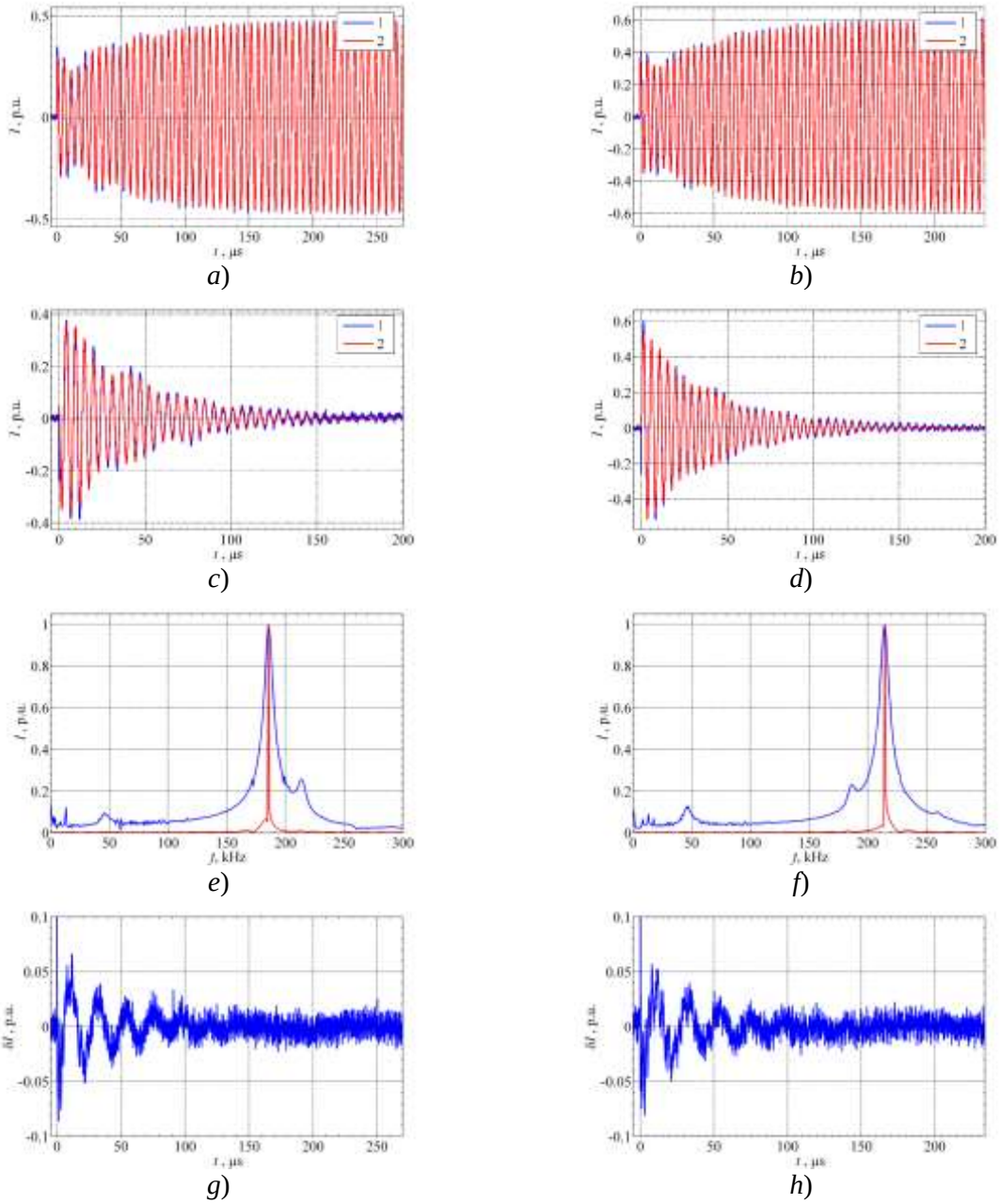

Figure 5 – Neutral transient current (a, b), approximation (c, d), frequency spectrum (e, f) and absolute fitting error (g, h) of free current component at frequencies of 186 (a, c, e, g) and 214 kHz (b, d, f, h)

It is evident from figure 5 that the neutral current contains component with a frequency of about 45 kHz which correspond to oscillations between HV and LV windings. It is important to note that oscillations at that frequency are not pronounced in the free voltage component spectrum of the HV winding middle point. Neglect of this oscillating component in the current led to an approximation error of about 10–15%. However, for estimation of frequencies and damping factors of self-

oscillations of the winding under consideration to take into account the inter-winding oscillation component is not of significant importance.

It is also evident from figures 5, g and 5, h that high-frequency noise is present in the neutral current signal which is due to small values of measured current – no more than 0,6·5 = 3 mA.

Obtained values of natural frequencies and damping factors are summarized in table 3 which also contains values of natural frequencies obtained from HV winding frequency responses in accordance with [7, 8].

Table 3 – Results of natural frequencies and damping factors determination

Parameters	Values for natural frequency with number	
	1	3
Natural frequency, kHz - from transient voltage approximation - from neutral current approximation - from active admittance in accordance with [7, 8]	 185,8 186,1 186,7	 214,4 214,9 214,3
Damping factors γ, 1/ms - from transient voltage approximation - from neutral current approximation	 21,9 21,1	 23,1 23,9
τ / *T* ratio - from transient voltage approximation - from neutral current approximation	 8,65 8,80	 9,29 8,97

Based on the results demonstrated above, it can be stated that approaches based on fitting of winding transient voltages and transient neutral current provide an acceptable degree of accuracy of natural frequencies and damping factors estimation for power transformers. An approach based on transient voltage fitting is more accurate due to higher signal-to-noise ratio, but it has certain limitations related to the availability of internal nodes in the measured winding which is not always possible in practice. An approach based on neutral transient current has lower signal-to-noise ratio and components related to inter-winding oscillations, however, it does not require the access to winding internal nodes which is an unquestionable advantage of this approach.

3. VERIFICATION AND IMPROVEMENT OF ACCURACY OF THE MODELS

In order to provide transformer windings ability to withstand resonant and high frequency overvoltages possible in operation, sufficiently accurate determination of internal insulation stresses under such conditions is needed at the design stage. This task can be solved in two steps:

1) calculation of voltage waveforms at transformer terminals during transients initiated by typical switching processes in renewable generation electrical network;

2) calculation of transformer windings internal insulation stresses caused by calculated voltage waveforms at transformer terminals.

Accurate calculation of resonant overvoltages is not possible without taking into account the frequency dependency of damping of oscillations inside transformer windings. Due to that, the inclusion of experimental values of damping factors obtained in accordance with recommendations of section 2 into transformer model used for simulation of transients both in external network and inside windings is needed. The method of such inclusion is described in this section.

3.1 Calculation of voltages at transformer terminals

Undamped transients inside transformer windings can be described using the following system of ordinary differential equations [5]:

$$\begin{cases} \dfrac{dU(t)}{dt} = -\mathbf{C}^{-1}\mathbf{T}^{T} I(t) - \mathbf{C}^{-1}\mathbf{C_0} \dfrac{dU_0(t)}{dt} \\ \dfrac{dI(t)}{dt} = \mathbf{L}^{-1}\mathbf{T}U(t) + \mathbf{L}^{-1}\mathbf{T_0}U_0(t) \end{cases}, \qquad (8)$$

where $U(t)$ is the vector of voltages at transformer equivalent circuit nodes; $I(t)$ is the vector of currents in transformer equivalent circuit branches; **L** is inductance matrix; **C** is capacitance matrix; **T** is incidence; $\mathbf{C_0}$ – matrix of capacitances between circuit internal nodes and external terminals; $\mathbf{T_0}$ – matrix representing connections between equivalent circuit branches and external terminals.

Natural frequencies of windings internal voltage oscillations can be obtained as the eigenvalues of system matrix of the ordinary differential equations system in relation to winding internal voltages. We now formulate such equations system by differentiating the first equation of (8) and considering the second equation of (8):

$$\frac{d^2U(t)}{dt^2} = -\mathbf{C}^{-1}\mathbf{T}^{T}\mathbf{L}^{-1}\mathbf{T}U(t) - \mathbf{C}^{-1}\mathbf{T}^{T}\mathbf{L}^{-1}T_0U_0(t) - \mathbf{C}^{-1}\mathbf{C_0}\frac{d^2U_0(t)}{dt^2}. \qquad (9)$$

System matrix eigenvalues

$$\lambda = \mathrm{eig}(\mathbf{M}) = \mathrm{eig}\left(-\mathbf{C}^{-1}\mathbf{T}^{T}\mathbf{L}^{-1}\mathbf{T}\right) \qquad (10)$$

represent the squares of transformer windings natural frequencies. We now take account of the frequency dependency of natural oscillations damping by correction of **M** eigenvalues:

$$\lambda' = \left(\left(\gamma/\omega\right)^2 - 1\right)|\lambda| - 2j\left(\gamma/\omega\right)|\lambda|, \qquad (11)$$

the ratio γ/ω being set in accordance with experimental data obtained using section 2 recommendations.

System matrix restoration using corrected eigenvalues is done as follows:

$$\mathbf{M}' = \mathbf{V}\mathbf{\Lambda}\mathbf{V}^{-1}, \qquad (12)$$

where $\mathbf{\Lambda}$ is the diagonal matrix of corrected eigenvalues λ' of matrix **M**; **V** is the matrix consisting of eigenvectors of **M**. Corrected system matrix **M'** allows one to simulate transients both in external network and inside transformer windings with taking account of the frequency dependency of natural oscillations damping.

Calculation of voltage waveforms at transformer terminals requires the use of the model representing transformer behavior as seen from the external network. Such models are called black-box models [1]; in the case of transformers these models are formulated using frequency response of terminal admittance matrix [15]. At the design stage, such models can be built via the calculation of the terminal admittance matrix using transformer design data. This approach allows one to take frequency dependency of damping into account by correction of system matrix of equations system (9) in accordance with (11). Calculation of frequency response of terminal admittance matrix is performed by means of solving the equations system (8) in the frequency domain:

$$\begin{cases} j\omega\dot{U}(\omega) = -\left(\mathbf{C}'\right)^{-1}\mathbf{T}^{T}\dot{I}(t) - j\omega\left(\mathbf{C}'\right)^{-1}\mathbf{C_0}\dot{U}_0(\omega) \\ j\omega\dot{I}(\omega) = \mathbf{L}^{-1}\mathbf{T}\dot{U}(\omega) + \mathbf{L}^{-1}\mathbf{T_0}\dot{U}_0(\omega) \end{cases}, \qquad (13)$$

where **C'** is corrected capacitance matrix calculated via corrected system matrix **M'**:

$$\mathbf{C}' = -\left(\mathbf{M}'\right)^{-1}\mathbf{T}^{T}\mathbf{L}^{-1}\mathbf{T}. \qquad (14)$$

Using (13), the frequency response of terminal admittance matrix $\mathbf{Y}(\omega)$ is calculated column-by-column: for calculation of j-th column, j-th element of the vector of terminal voltages $U_0(\omega)$ should be

equal to unity, the other elements being equal to zero. After solving (13) the frequency response of j-th column of $\mathbf{Y}(\omega)$ is calculated as follows:

$$\dot{Y}_j(\omega) = j\omega \mathbf{C}_0^T \dot{U}(\omega) + \mathbf{T}_0^T \dot{I}(\omega). \qquad (15)$$

The frequency response of the terminal admittance matrix of 630 kVA dry-type transformer is shown in figure 6; the frequency dependency of the damping is taken into account in accordance with (10–12). The values of damping factors are calculated in accordance with section 2 recommendations.

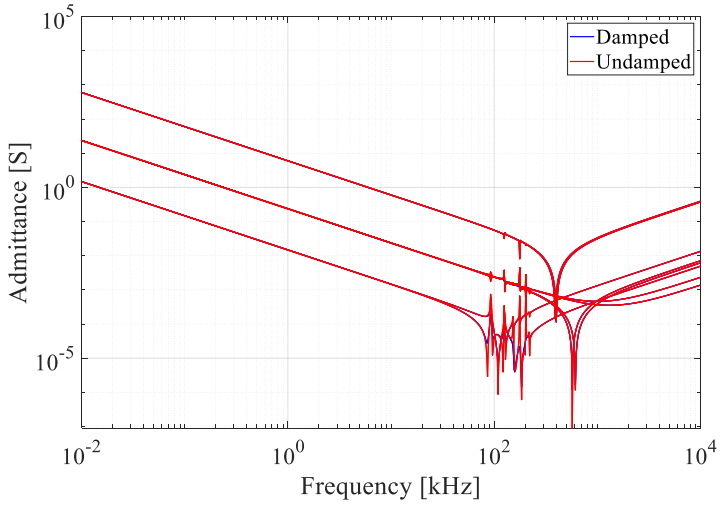

Figure 6 – Damped and undamped frequency responses of terminal admittance matrix of 630 kVA dry-type transformer

Black-box model is formed by means of the approximation of calculated frequency responses. Inclusion of obtained transformer model into renewable generation network model is implemented using obtained approximation coefficients [16].

3.2 Calculation of internal insulation stresses inside windings

Voltage waveforms at transformer terminals calculated using the black-box model described in sub-section 3.1 are the input data for calculation of internal insulation stresses inside transformer windings. Calculation of voltage transfer from transformer terminals to selected internal nodes is performed using corresponding transfer functions.

Calculation of transfer function can be performed via solving of equation (9) in the frequency domain:

$$\dot{U}(\omega) = \left(\mathbf{M}' - \omega^2 \mathbf{I}\right)^{-1} \left(\omega^2 \mathbf{C}^{-1}\mathbf{C}_0 - \mathbf{C}^{-1}\mathbf{T}^T\mathbf{L}^{-1}\mathbf{T}_0\right)\dot{U}_0(\omega), \qquad (16)$$

where $\mathbf{I}$ – is the identity matrix. Figure 7, a shows the comparison of transfer functions of the middle point of HV winding calculated using (16) and obtained experimentally.

With known voltage waveforms at transformer terminals, selected internal nodes voltages can be calculated using coefficient of corresponding transfer functions approximation:

$$\begin{cases} \dfrac{dX(t)}{dt} = \mathbf{A}X(t) + \mathbf{B}U_0(t), \\ U_{\text{int}}(t) = \mathbf{C}X(t) + \mathbf{D}U_0(t) \end{cases} \qquad (17)$$

where $U_{\text{int}}(t)$ is the vector of voltages at selected internal nodes; $\mathbf{A}$, $\mathbf{B}$, $\mathbf{C}$, $\mathbf{D}$ – matrices containing coefficients of transfer functions approximation. Figure 7, b shows the comparison of simulated and registered voltage waveforms of the middle point of 630 kVA dry-type transformer HV winding under the impact of sinusoidal voltage with frequency equal to the first natural frequency of HV winding.

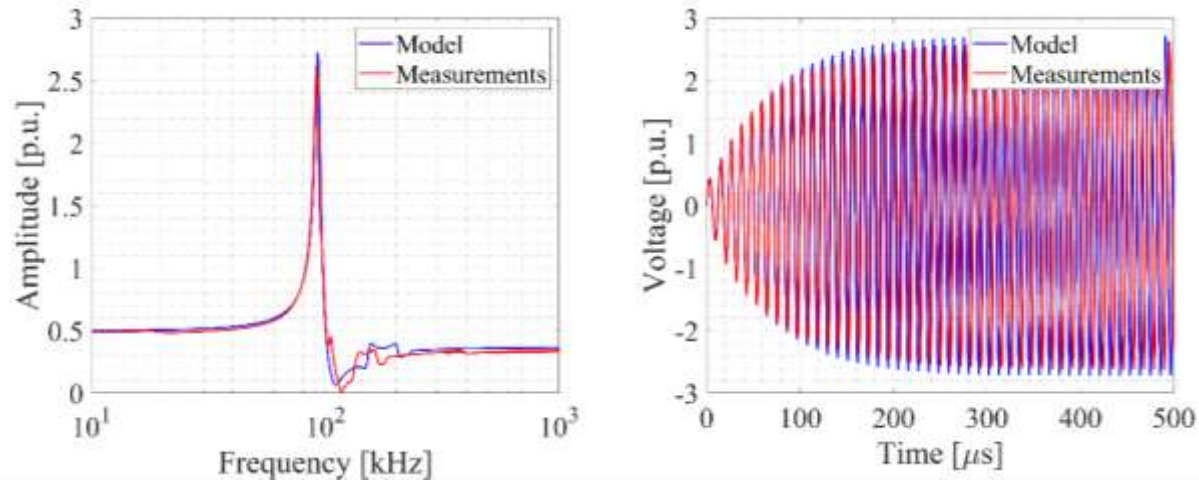

a) *b)*

Figure 7 – Transfer function of voltage (a) and voltage waveform (b) at HV winding middle point of 630 kVA dry-type transformer with sinusoidal voltage with frequency equal to the first natural frequency of HV winding applied to HV winding line terminal

Comparison of the first natural frequency of HV winding and resonant voltage rise in winding middle point obtained by the model with experimental values is presented in table 4.

Table 4 – Comparison of model and experimental data regarding the first natural frequency of 630 kVA dry-type transformer HV winding

Parameter	Calculated	Measured	Difference, %
First natural frequency of HV winding, kHz	92,7	91,7	1,1
Resonant voltage rise at the first natural frequency of HV winding, p.u.	2,73	2,62	4,2

4. WIDEBAND TRANSFORMER MODEL

Renewable generation systems commonly comprise power electronics converters that connect DC networks of wind generators and photovoltaic cells with AC power utility system. In recent years, solid-state transformer technology got significant development; this technology finds application in the renewable generation systems. Transformers in such converter units operate in non-standard conditions: voltage waveforms are often non-sinusoidal, and operational mode represent the periodical sequence of transients initiated by power converters switching. Numerical modeling of such units requires the application of wideband transformer model which would be correct for the simulation of both low-frequency and high-frequency transients as well as steady states.

To be correct at high frequencies, the model should have detailed representation of windings. The main disadvantage of classical detailed transformer models (white-box models) is an inability to represent low-frequency phenomena correctly. Historically, such models were used for impulse transients simulation inside transformer windings. For that application, it is acceptable to neglect magnetization phenomena; in the meantime, magnetization should be taken into account during the simulation of quasi-steady-state modes of converter units.

The suggested wideband model is based on a detailed equivalent network of the transformer [17]. For the sake of simplicity, the model shown in figure 8 represents a two-winding transformer, each of the windings being split into four elements. For each of the elements the set of parameters is calculated: self and mutual inductances, series capacitance, capacitance to the ground and nearby winding, the

resistance of the part of winding represented by the given element. Self and mutual inductances of winding parts are taken into account in transformer equivalent network by means of series and shunt inductances which are calculated using inductive decoupling. For the sake of simplicity, in figure 8 notations are given only for those parameters of an equivalent network which are related to element with the number 1.

The whole set of series and shunt inductances is the electric equivalent network of the magnetic circuit of the transformer which is separated from the rest of the equivalent circuit by ideal transformers. For convenience, inductances are referred to unity number of turns; this allows to use the number of turns of the element as the corresponding ideal transformer ratio.

The equivalent circuit may be supplemented by resistances representing core losses; for the sake of simplicity that resistances are not shown in the figure.

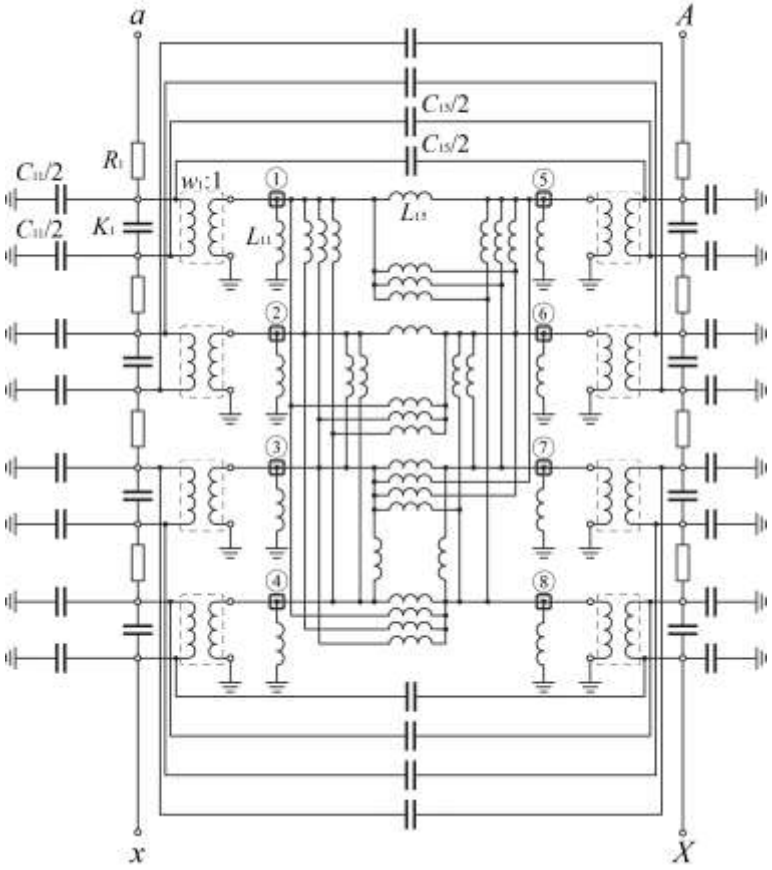

L_{ii} – shunt inductance of electric euivalent network of transformer magnetic circuit; L_{ij} – series inductance; K_i – series capacitance of winding element; C_{ii} – capacitance of winding element to ground; C_{ij} – capacitance bwtween elements of transformer winding; R_i – resistance of winding element; w_i:1 – ideal transformer; *a*, *x* – linear and neutral terminals of LV winding; *A*, *X* – linear and neutral terminals of HV winding

Figure 8 – Wideband equivalent circuit of the transformer

The distinctive feature of the suggested model is the fact that series and shunt inductances of equivalent circuit are considered with taking account of transformer core magnetization. As a results, the model turns out to be correct for the calculation of linear low-frequency and steady-state phenomena which require the modeling of magnetization. In the meantime, this model is capable of correct representation of transformer natural frequencies; the more detailed the windings representation is, the higher are the natural frequencies that can be represented by the model. Another advantage of the model is the fact that winding splitting into parts allows one to calculate dielectric stresses on different parts of internal insulation; this is especially crucial for transformers in converter units, internal insulation of which is commonly affected by voltage with non-standard waveforms often containing DC components.

Verification of suggested wideband transformer model can be implemented both in frequency and in the time domain: for example, by means of comparison of frequency responses of input admittance or transfer functions in typical operational arrangements as well as by means of comparison of simulated and registered waveforms of currents and voltages in operation mode. The example of the development and verification of such a model is presented in [17].

CONCLUSIONS

Development of methods for experimental determination of power transformers windings natural frequencies and damping factors plays an important part in improvement and verification of high-frequency transformer windings mathematical models applicable for resonant overvoltages simulation.
Verified high-frequency models can be obtained with the use of experimental data on natural frequencies and damping factors.
Natural frequencies and damping factors of power transformer windings can be determined approximately using voltage transfer functions of windings internal nodes available for measurements as well as analyzing resonance peaks width of winding frequency responses.
Natural frequencies and damping factors also can be obtained using an approach implying registration of winding transient voltages and currents, extraction of free components of oscillations and subsequent spectral analysis and time-domain approximation using analytical equations describing free oscillations in windings.
Damping factors obtained experimentally can be included in numerical models of transformers via eigenvalues correction of matrix of equations system describing transients inside windings. The corrected matrix can be used for calculation of terminal admittance matrix frequency response as well as for calculation of voltage transfer functions between transformer terminals and selected internal nodes of the winding. Model is formulated based on calculated frequency responses fitting; this model takes experimentally obtained damping factors into account in case of simulation both external network transients and transients inside transformer windings.
An approach to the development of a wideband transformer model correct for both high-frequency and low-frequency transients as well as for steady-state modes is presented. The distinctive feature of the suggested model is the possibility of taking core magnetization into account while preserving detailed representation of windings. Such models may be especially useful in the design process of transformers for operation in non-standard conditions, for example, in the case of transformers for renewable generation.

BIBLIOGRAPHY

[1] CIGRE Technical Brochure 577A. “Electrical Transient Interaction between Transformers and the Power System – Part 1: Expertise”. Joint Working Group A2/C4.39, April 2014. ISBN: 978-2-85873272-2.

[2] B. Gustavsen, A. Portillo. A Damping Factor-Based White-Box Transformer Model for Network Studies // IEEE Transactions on Power Delivery, 2018, Vol. 33, No. 6, PP. 2956 – 2964. DOI: 10.1109/TPWRD.2018.2847725.

[3] B. Gustavsen, C. Martin, A. Portillo. Time-Domain Implementation of Damping Factor White-Box Transformer Model for Inclusion in EMT Simulation Programs // IEEE Transactions on Power Delivery, 2020, Vol. 35, No. 2, PP. 464–472. DOI: 10.1109/TPWRD.2019.2902447.

[4] P.I. Fergestad, T. Henriksen. Transient Oscillations in Multiwinding Transformers // IEEE Trans. on Power Apparatus and Systems, Vol. 93, No. 2, 1974, p. 500-509.

[5] Calculation of impulse stresses in transformer windings on a computer / Z.M. Beletsky et all // Moscow: Informelectro, 1978 (in Russian).

[6] V.S. Larin, D.A. Matveev, B.K. Maximov. Resonant overvoltages inside power transformer windings and the measures improving their ability to withstand high-frequency stresses // 48th CIGRE Session, report A2-203, Paris, France, 24 August – 3 September 2020.

[7] V. Larin, D. Matveev, A. Volkov. Study of transient interaction in a system with transformer supplied from network through a cable: assessment of interaction frequencies and resonance

evolvement // Proceedings of the 3rd International Colloquium Transformer Research and Asset Management, Split, Croatia, October 15 – 17, 2014.
[8] CIGRE Technical Brochure 812. Advances in the interpretation of transformer Frequency Response Analysis (FRA). CIGRE Working Group A2.53, September 2020. ISBN: 978-2-85873-517-4.
[9] IEC 60076-18:2012 Power transformers - Part 18: Measurement of frequency response. ISBN 978-2-83220-222-7.
[10] V.S. Larin, D.A. Matveev, A.Yu. Volkov. Application of power transformer winding admittance measurements for FRA interpretation // Proceedings of International Colloquium on Latest Trends and Innovations on Power Transformers & Reactors, Overhead Lines and Materials and Emerging Test Techniques (Under the aegis of CIGRE SC A2 on Transformers; B2 on Overhead Lines and D1 on Materials), 21-22 November 2019, New Delhi, India. PP. A2-190 – A2.197.
[11] Nilsson, James, and Susan Riedel. Electric Circuits, Global Edition. 11th ed. Pearson, 2019.
[12] Larin V.S., Matveev D.A. Determination of Damping Factors Based on the Measured Frequency Responses of Power Transformer Windings. Part 1. Theoretical Consideration // Electrichestvo, 2021, No. 1, pp. 13–22. (in Russian). DOI:10.24160/0013-5380-2021-1-13-22.
[13] Larin V.S., Matveev D.A. Determination of Damping Factors Based on the Measured Frequency Responses of Power Transformer Windings. Part 2. Analysis of Measurement Results // Electrichestvo, 2021, No. 2, pp. 22–28. (in Russian). DOI:10.24160/0013-5380-2021-2-22-28.
[14] Larin V.S., Matveev D.A. Approximation of Transient Resonant Voltages and Currents in the Power Transformer Windings to Determine the Natural Frequencies and Damping Factors // Electrichestvo, 2020, No. 12, pp. 44–54. (in Russian). DOI:10.24160/0013-5380-2020-12-44-54.
[15] B. Gustavsen. Wide Band Modeling of Power Transformers // IEEE Transactions on Power Delivery, 2004, Vol. 19, No. 1, PP. 414–422. DOI: 10.1109/TPWRD.2003.820197.
[16] B. Gustavsen, A. Semlyen. Rational Approximation of Frequency Domain Responses by Vector Fitting // IEEE Trans. on Power Delivery, Vol. 14, No. 3, 1999, PP. 1052-1061. DOI:10.1109/61.772353.
[17] Zhuikov A.V., Kubatkin M.A., Matveev D.A., Frolov M.V., Khrenov S.I., Larin V.S., Nikulov I.I. A Broadband Model of Step-up Transformers for High-Frequency Power-Supply Units of Electrostatic Precipitators. Russ. Electr. Engin. 92, 200–208 (2021). https://doi.org/10.3103/S1068371221040106